International Journal for Housing Science and Its Applications
Publish August 6, 2025. Volume 46, Issue 3 Pages 7521-7533

https://doi.org/10.70517/ijhsa463645

Mechanism of termination of Na+ current elimination-induced oscillations in response to external noise stimulation

Xiaoqin Si[1,*] and Dawei Chen[1]
[1] City University of Hefei, Hefei, Anhui, 238076, China
Corresponding authors: (e-mail: sxq0796@163.com).

Abstract Modern living environments expose humans to various types of noise for long periods of time, which may come from environmental exposures, geomagnetic environments, communication equipment, and electrical equipment. Acoustic stimulation, a non-invasive neurological disease treatment, has been shown to have specific effects on the human nervous system. The present study investigated the mechanisms by which external noise stimulation affects ion channel properties in neuronal cells. Whole-cell membrane clamp technique was used to record ion channel current changes in rat cortical neurons under external noise stimulation, and ion channel kinetic properties were analyzed in conjunction with the Hodgkin-Huxley model. The experimental results showed that the external noise environment increased the peak Na+ channel current density, which increased from -263.22±38.47 pA/pF in the control group to -372.83±11.09 pA/pF after 18 min of noise stimulation. Meanwhile, the external noise stimulation significantly inhibited the transient outward potassium current, and the percentage of inhibition increased with the prolongation of the stimulation time, reaching 62.62% at 18 min. It reached 62.62% at 18 min. Further analysis revealed that the external noise stimulation left shifted the half-activation voltage of Na+ ion channels from -32.04±0.58 mV to -56.42±0.51 mV, which promoted the activation process of Na+ channels; meanwhile, it left shifted the half-inactivation voltage of Na+ currents from -30.21±0.19 mV to -50.52±0.75 mV, which accelerated the Na+ ion channel inactivation rate. The study reveals the mechanism by which external noise stimuli change the oscillatory properties of neurons by affecting the properties of ion channels, and provides a cellular level experimental basis for understanding the effects of noise environment on the nervous system.

Index Terms External noise stimulation, Ion channel, Membrane clamp technique, Na+ current, Transient outward potassium current, Neuronal oscillation

I. Introduction

The brain is an important material basis for human understanding of self, and there are only 1011 neurons in the human brain by and large, much less than the number of non-neuronal cells such as glial cells [1]. However, neurons are unique because only they can transmit electrical signals over long distances [2]. As the basic unit of structure and function of the nervous system, the neuron, its firing behavior is closely linked to the utility of the organism's sectoral systems [3], [4]. From the neuronal level accessible to neuronal circuits, to cortical structures, to the whole brain and finally to the behavior of the organism, the study of neuronal dynamical behavior is important for the understanding of the behavior of the organism [5]-[7].

The phenomenon of resonance occurs when the vibration frequency of one object is the same or close to the intrinsic frequency of another object [8]. The nervous system of an organism, as a typical nonlinear system, can produce similar resonance phenomena in response to external forces [9]. Neurons stimulated by appropriate noise can respond greatly to weak signals, i.e., stochastic resonance, or the firing activity can be maximally suppressed, i.e., anti-stochastic resonance [10], [11]. It is well known that most of the neuronal models developed so far are dominated by the effect of ion channel currents on the generation of membrane potentials [12]. The efflux of ions out of the cell membrane through ion channels as well as the pumping of ions into the cell membrane through the endoplasmic reticulum generates ionic currents that simultaneously cause fluctuations in the electric and magnetic fields inside and outside the membrane [13]-[15]. In addition to physiological experimental exploration, numerical computation and theoretical analysis of neuronal model signal stimuli are also effective to explore their kinetic response behavior [16], [17]. It can theoretically guide the experiments and provide some insights into the physiological responses resulting from the stimulus signals [18].

Bioelectrical activity is the basis of information transmission in the nervous system, and ion channels, as transmembrane proteins, play a key role in membrane potential changes and action potential generation in neuronal cells. By selectively controlling the transmembrane flow of various types of ions, ion channels participate in and

regulate the basic physiological activities of neurons. Information exchange between neurons is mainly realized by action potentials, the generation and propagation of which depend on the concerted work of multiple ion channels, especially voltage-gated sodium and potassium channels. These channels undergo changes in their switching state in response to external stimuli, thus affecting the fluctuation of cell membrane potential. In recent years, it has been found that environmental noise may affect the function of the nervous system through a variety of pathways, including altering neuronal excitability, influencing synaptic transmission between neurons, and modulating the oscillatory activity of neural networks. However, the direct effects of environmental noise on ion channel current properties and their cellular mechanisms have not been fully elucidated. From a clinical perspective, a large number of neurological disorders are associated with ion channel dysfunction, such as epilepsy, chronic pain, and neurodegenerative diseases. Therefore, an in-depth understanding of the relationship between noise stimulation and ion channel function not only helps to reveal the mechanism of the influence of environmental factors on the nervous system, but also provides new ideas for the treatment of related diseases. In particular, the elucidation of the mechanism of action of acoustic stimulation as a noninvasive neuromodulation means is of great significance for the development of novel neuromodulation techniques.

In this study, we used the membrane clamp technique for electrophysiological recordings of rat cortical neurons, and systematically investigated the effects of external noise stimulation on the current characteristics of sodium ion channels and potassium ion channels, including current density, activation curves, inactivation curves and other parameters. By establishing a simulated motion acoustic stimulation system, the effects of noise stimulation with different parameters on ion channel properties were investigated, and their time-dependence and voltage-dependence were analyzed. Meanwhile, the bifurcation mechanism of neuronal oscillatory behavior under noise stimulation was explored by combining with the ion channel kinetic model to reveal the kinetic mechanism by which external noise affects neuronal firing activity. This study not only helps to understand the mechanism of environmental noise on the nervous system, but also provides a theoretical basis for the development of neuromodulation technology based on acoustic stimulation, which is of great significance to the study of neuroelectrophysiology and the treatment of neurological diseases.

II. Relevant theoretical and technical foundations

Modern lifestyles expose humans to noise almost all the time, especially very low noise environments. People are becoming more and more dependent on different types of electronics, and environmental exposures, geomagnetic environments, communication equipment and electrical equipment are all important sources of noise generation. The use of acoustic stimulation as a noninvasive method for the treatment of neurological disorders suggests that acoustic stimulation does have some effect on human nerves. However, the effects of external noise stimulation on the characteristics of microscopic cell point activity and the mechanism of action have not yet been conclusively determined, which is a hot concern of current researchers.

II. A. Diaphragm clamp technology

II. A. 1) Principles of diaphragm clamp technology

Membrane clamp technology is through the glass microelectrode and the cell membrane to form a high-resistance sealing (sealing resistance in the gigaohm to tens of GΩ), so that the sealing of the membrane and the rest of the cell membrane is completely isolated electrically, and then through the glass microelectrode by applying a negative pressure on the electrode tip of the electrode at the tip of the small piece of the membrane is suction broken into the electrode. At this time, the edge of the glass electrode tip and the periphery of the small piece of membrane form a high-resistance sealing, the sealing resistance can reach a few G ohms, electrically isolating the broken small piece of membrane and the surrounding membrane, and the current recorded by the electrode is only related to the state of the channel on the membrane. At this point, depending on the recording mode, the current can be either a whole-cell current or a single-channel current (the clamped diaphragm contains only one or a few channel proteins) [19].

Figure 1 shows the principle structure of a membrane clamp amplifier, where a field effect tube operational amplifier constitutes the I-V converter, i.e. the pre-probe of the membrane clamp amplifier.

The positive and negative input terminals of the FET operational amplifier are equipotential, and a command voltage is added from its positive input terminal, and the voltage applied to the diaphragm can be constant according to the "virtual break" and "virtual short" phenomenon of the negative feedback amplification circuit, so as to achieve the purpose of potential clamping. When the sealing resistance R_{seal} is as high as $G\Omega$, we can get $I_{rho} / I = R_{seal} / (R_x R_{seal}) - 1$, under the action of the command voltage V_c, the voltage drop generated by the current I_ρ through the negative feedback resistance R_f meets $V_{o1} - V_c = -I_p R_f$, and then pass through the unit difference

amplifier circuit A_2 to obtain $V_o = I_p R_f$. Due to the high resistance of the electrode and the diaphragm, the shunt of the sealing resistance is minimized, and the current I_p can be approximated as the current I across the diaphragm [20].

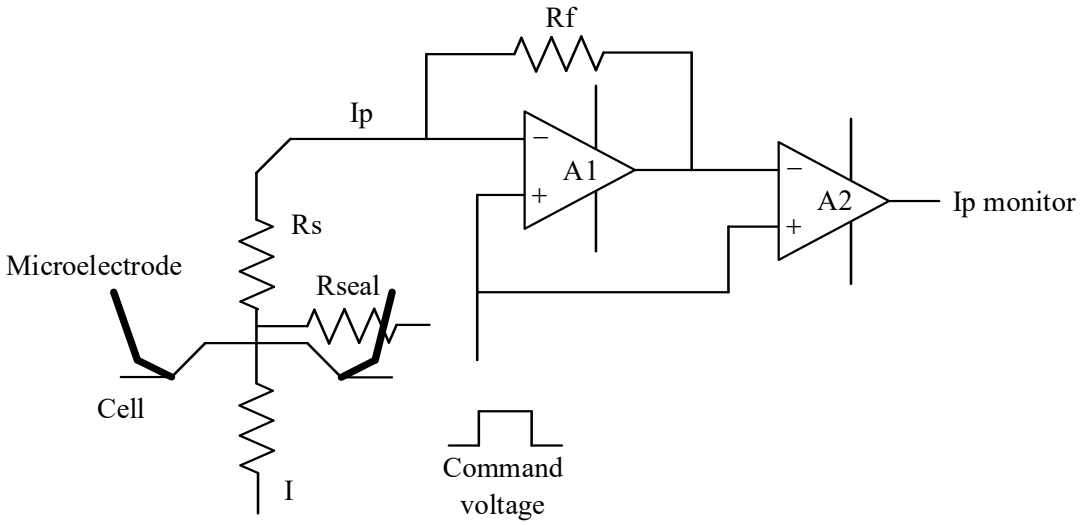

Figure 1: The principle and structure of the diaphragm clamp amplifier

II. A. 2) Membrane clamp recording mode

(1) Single-channel recording method - cell adsorption mode

After the microelectrode is close to the cell under the microscope, a negative pressure is applied to the microelectrode to form a high impedance seal. At this time, it can be seen that the background noise is significantly reduced, and the membrane sheet with only one channel under the electrode is usually selected for analysis, i.e., single-channel recording, in order to facilitate the observation of the activity state of one channel without distortion. The advantage of this method is that it minimizes interference with the cell membrane structure and modulation system, and can accurately reflect the activity state of the channel and objectively analyze it. The disadvantage is that the current is small, the resolution is low, the technical requirements are high, the difficulty is large and the workload is large and the success rate is low.

(2) Whole cell recording method

In the high impedance sealing is done, and then give a very small negative pressure, the electrode covering the membrane suction broken, so that the electrode and the whole cell connected, with this method can be recorded in and out of the whole cell current. The advantage of this method is that the current is large, the signal-to-noise ratio is good, can do both current clamping and voltage clamping, and can change the cell contents. However, this method can only be used for cells with a diameter of less than 3μ, and can only observe changes in membrane currents, and cannot analyze the mechanism of change generation.

(3) Outside-in - Inside-out mode

These two techniques are improved on the basis of cell-adherent and whole-cell recording, respectively, with the advantage that the effects of chemical factors on the structure of the inner and outer sides of the cell membrane can be observed separately. When the electrode is lifted from the cell, the cell membrane connected to the electrode tip is torn off to form a vesicle, and the vesicle ruptures soon after exposing the electrode tip to the air to form an inside-out membrane with the cytoplasmic side facing outward. Outside to the outside is the formation of cell-adherent membrane sheet, the pipette electrode to give a strong negative pressure will be suction broken membrane sheet, and then the electrode will be pulled up from the cell membrane, was torn off the membrane will be formed outside to the outside of the membrane sheet.

II. B.Assumptions underlying neuronal coding

II. B. 1) Action potentials and ion channels

(1) Action potential

Action potential is a process in which the membrane potential fluctuates on the basis of the resting potential after receiving an effective stimulus, which is characterized by a rapid rise to the peak and then a slow return to the quiet state. A complete action potential release process consists of three parts, namely, depolarization, repolarization,

and posthyperpolarization. Depolarization is the process by which the resting potential increases and is reflected in the rising edge of the action potential. Repolarization is the process in which the membrane potential changes in the direction of the resting potential, which is reflected in the falling edge of the action potential. Post-hyperpolarization is a slow process in which the membrane potential returns to the quiet state. The action potential release is schematically shown in Figure 2, and the whole process is very short. It has been demonstrated that the waveforms of action potentials tend to carry a wide variety of information, and the process is encoded by the peaks and frequencies realized by neural coding [21].

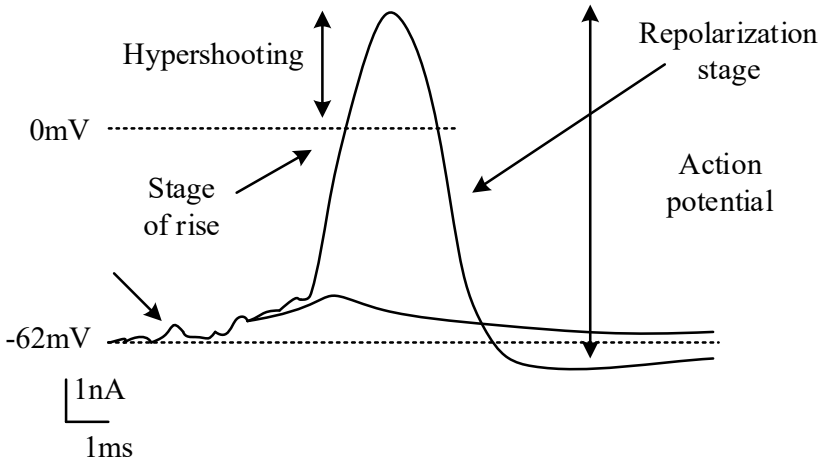

Figure 2: Neuronal action potential diagram

Normally a stimulus of a certain intensity is required to cause a neuron to trigger an action potential, and the minimum stimulus intensity at which an action potential can be triggered is known as the threshold of the stimulus. Stimulation below the threshold does not generate an action potential, but after the stimulus reaches the threshold an action potential is triggered, and continuing to increase the intensity of the magnetic stimulus has no effect on the amplitude of the action potential. For a single neuron, the triggered action potential maintains a relatively constant waveform and amplitude, a characteristic known as the “all” or “nothing” phenomenon.

Action potentials are in the form of electrical impulses, which are triggered by stimulation in a certain part of the neuron, and its local membrane potential rapidly changes to an internal positive and external negative state due to excitation, forming a battery effect. The neighboring parts of the neuron are still at resting potential, which rapidly constitutes a broad stimulus, causing the neighboring parts to enter an excited state one after another and generating action potentials in the form of electrical impulses. The action potential in the local membrane of the neuron confirms that the neighboring parts are triggered to generate action potentials sequentially through this local current mechanism. Action potentials have the characteristics of “all” or “none”, so the amplitude and waveform do not change during conduction depending on the distance.

(2) Ion channels

Excitement in the motor neuron in the form of action potential, regulated by ion channels, ion channels are embedded in the phospholipid bilayer protein structure, mainly responsible for the transportation of charged ions inside and outside the cell, of which sodium (Na +), potassium (K +), chlorine (Cl -) three kinds of ions on the generation of action potential plays a major role.

Taking the motor neuron of rat as an example, when the cell membrane is in the resting state, the concentration of Na+ and Cl- in the extracellular fluid is greater than that in the intracellular fluid, while the concentration of K+ is less than that in the intracellular fluid, resulting in a potential of about -50mV in the cell membrane in the resting state. When the ion channel is opened, Na+ inward flow and K+ outward flow lead to depolarization of the membrane voltage to form an action potential, and when the action potential is over, the ion channel is closed, the sodium-potassium pump carries the excess Na+ and K+ in the reverse direction, and the membrane potential is restored to the resting state. Ion channels are divided into two types: voltage-gated and ligand-gated. The opening and closing of voltage-gated ion channels is mainly affected by the voltage difference between the inside and outside of the membrane, such as sodium and potassium channels, while the ligand-gated type requires specific types of ions to bind to the receptor in order to be opened, such as calcium-dependent potassium channels.

II. B. 2) The Hodgkin-Huxley model

The Hodgkin-Huxley fourth-order differential equation (H-H model) is a classical mathematical model describing the ionic currents in the giant axon of the gun squid, which can help to understand the molecular structure and mechanism of action of the ion channels, and it was proposed on the basis of many experimental data. Through voltage-clamp experiments, the former found that a sudden change in membrane potential from the equilibrium position to the depolarization level would be followed by a transient inward current and then an outward current for a sustained period of time, and further proved that the ionic currents and membrane voltage obeyed Ohm's law through the measurement of the tail current method [22]. For the potassium ion channel only activation gates exist, and the activation gates are four can get the better fitting results. The H-H equation is obtained by deriving the evolution of a series of functions as follows:

$$C_m \frac{dV}{dt} = -G_K n^4 (V - V_K) - G_{Na} m^3 h (V - V_{Na}) - G_L (V - V_L) \tag{1}$$

$$\frac{dy}{dt} = \alpha_y (1 - y) - \beta_y y, (y = n, m, h) \tag{2}$$

$$\begin{cases} \alpha_n = \dfrac{0.01(V+55)}{1-\exp[-(V+55)/10]}, \beta_n = 0.125\exp[-(V+65)/80] \\ \alpha_m = \dfrac{0.1(V+40)}{1-\exp[-(V+40)/10]}, \beta_m = 4\exp[-(V+65)/18] \\ \alpha_h = 0.07\exp[-(V+65)/20] \beta_h = \{1+\exp[-(V+35)/10]\}^{-1} \end{cases} \tag{3}$$

where C_m represents the capacitance of the neuronal membrane, V represents the neuronal membrane potential, V_K, V_{Na} and V_L represent the reversal potentials of the potassium, sodium and chloride channels, respectively, G_K, G_{Na} and G_L represent the maximum conductance of the three ion channels, and n, m and h represent the maximum conductance of the three ion channels, respectively The activation rate of potassium channel, sodium channel activation and inactivation are denoted respectively, and the opening and closing rates of ion channels are represented by α_y and β_y, respectively. The H-H model is the most basic model to study the behavior of neuronal firing activity, which provides the basis and foundation for subsequent in-depth investigation of neuroelectrophysiological properties.

Under the environment of external noise stimulation, the decrease in the number of ion channels caused by the increase in the corresponding channel noise component, so it is also necessary to consider the channel noise generated by the stochastic properties of ion channel dynamics. The H-H model considering ion channel blockage and channel noise is as follows:

$$C_m \frac{dV}{dt} = -G_K x_K n^4 (V - V_K) - G_{Na} x_{Na} m^3 h (V - V_{Na}) - G_L (V - V_L) \tag{4}$$

$$\frac{dy}{dt} = \alpha_y (1 - y) - \beta_y y + \xi_y(t), (y = n, m, h) \tag{5}$$

$$\begin{cases} \langle \xi_m(t) \xi_m(t') \rangle = \dfrac{2}{N_{Na} x_{Na}} \dfrac{\alpha_m \beta_m}{[\alpha_m + \beta_m]} \delta(t - t') \\ \langle \xi_h(t) \xi_h(t') \rangle = \dfrac{2}{N_{Na} x_{Na}} \dfrac{\alpha_h \beta_h}{[\alpha_h + \beta_h]} \delta(t - t') \\ \langle \xi_n(t) \xi_n(t') \rangle = \dfrac{2}{N_K x_K} \dfrac{\alpha_n \beta_n}{[\alpha_n + \beta_n]} \delta(t - t') \end{cases} \tag{6}$$

where the parameters x_k and x_{Na} denote the blockage rate of potassium and sodium ion channels, respectively, i.e., the ratio coefficient of the number of non-blocked ion channels to the total number of ion channels, i.e., the smaller the coefficient of this ratio is, the greater the degree of blockage is. The $\xi_v(t)$ denotes the random variable of statistical properties i.e. the noise of each ion channel, and the noise in this model belongs to Gaussian white noise. The N_{Na} and N_k in the voice expression denote the total number of sodium channels and the total number of potassium channels, respectively, with sizes $N_{Na} = \rho_{Na} \times S$ and $N_k = \rho_k \times S$, respectively, where S is the membrane patch area size. From the point of view of statistical physics, the ion channel noise decreases with the increase of S, so the intensity of ion channel noise can be characterized by the membrane patch area S.

II. B. 3) Stochastic Chay Model for Channel Noise

The source of ion channel noise encompasses several aspects, and here we can make certain assumptions based on the kinetic behavior of ion channels. We consider that ion channel noise is caused by a stochastic leap in the opening and closing of the ion channel, and it is due to the generation of this internal neuronal noise, which adds stochastic fluctuations to the ionic conductance and ultimately leads to the generation of complex discharge rhythms [23].

This stochastic leap process is considered to be a Markov process and the corresponding polynomial for the ion channel noise can be referenced in the following equation:

$$\eta = \xi(t)\frac{1}{\sqrt{N}}\sqrt{\frac{2}{\tau_p(V)}p(1-p)} \tag{7}$$

where $\xi(t)$ is Gaussian white noise with mean 0 variance 1, $\tau_p(V)$ is the relaxation time, N the number of ion channels, and p is the probability of an ion channel opening. In order to portray a more realistic and biologically meaningful model of neuronal firing, the effect of channel noise on neuronal firing can be investigated by starting from ion channels.

The K^+ channel Gaussian white noise is added to the equations of the deterministic Chay model equation set to constitute the stochastic Chay model based on fast K^+ channel Gaussian white noise as follows:

$$\begin{aligned}\frac{dV}{dt} &= g_I m_\infty^3 h_\infty (V_I - V) + g_{K,V} n^4 (V_K - V) \\ &+ g_{K,C}\frac{C}{1+C}(V_K - V) + g_L(V_L - V)\end{aligned} \tag{8}$$

$$\frac{dn}{dt} = \alpha_n(V)(1-n) - \beta_n(V)n + \eta_n(t) \tag{9}$$

$$\eta_n = \xi_n(t)\frac{1}{\sqrt{N_K}}\sqrt{\frac{2}{\tau_n(V)}n(1-n)} \tag{10}$$

$$\frac{dC}{dt} = \rho(m_\infty^3 h_\infty (V_C - V) - K_C C) \tag{11}$$

When the Gaussian white noise $\xi_n(t)$ in Eq. (10) is replaced by Gaussian color noise $\sigma(t)$, it constitutes a stochastic Chay model based on fast K wide-channel Gaussian color noise.

III. Experimental materials and methods

The wide range of differences exhibited in cellular functions may be attributed to their different morphology and the nature and distribution of ion channels in the cell membrane. Neurocomputational scientific analysis methods in previous results are not very mature in terms of theoretical foundations and experimental conditions for the study of complex phenomena in biological nervous systems. Therefore, in this paper, with the help of the mode of processing information between neuronal cells, we study the nonlinear dynamics characteristics under external noise stimulation by imitating the neuronal information processing mechanism as well as the behavioral characteristics of neuronal networks.

III. A. Experimental materials

III. A. 1) Laboratory animals and reagents

The experimental animals were male SD rats, whose age was 15~20 days, provided by the Institute of Hygiene and Environmental Medicine, Chinese Academy of Medical Sciences. The animals were housed in single cages in a room temperature (21℃~26℃) incubator. The hippocampal region of SD rats at this growth period was fully developed and the skull was easily separated. The number of mice used in the experiment was minimized as much as possible, and this experimental procedure complied with the requirements of the Code of Ethics for Animals.

The drugs and reagents mainly included N-1hydroxyethylpiperazine-N-2-ethanesulfonic acid (HEPES), sodium adenosine triphosphate (Na2ATP), tetrodotoxin (TTX), tetraethylamine chloride (TEA-C1), cadmium chloride (CdCl2), ethyleneglycol-bis(aminoethyl)tetraacetic acid (EGTA), analytically pure 4-aminopyridine (4-AP), tetraethylamine chloride (TEA-Cl), and all other drugs were used. Cl), and all other drugs were domestic analytical pure.

The solutions required for the experiments were prepared as follows:

Artificial cerebrospinal fluid (ACSF) : Glucose 12 mM, NaHCO3 20 mM, KCl3 mM, MgCl2 1.5 mM, NaCl 100 mM, NaH2PO4-2H2O 1.2 mM, CaCl2 2.5 mM, control the PH value between 7.1 and 7.5, artificial cerebrospinal fluid was added with a 97%O2/3%CO2 gas mixture, and the solution was ready to use.

Na+ channel currents were recorded in artificial cerebrospinal fluid. 4-AP 1.5 mmol, CdCl2 0.2 mmol, and TEA-Cl 35 mmol were mixed into the artificial cerebrospinal fluid.

Standard extracellular fluid. KCl3 5.5 mmol/L, Glucose 12 mmol/L, MgCl2 1 mmol/L, NaCl 100 mmol/L, HEPES 12 mmol/L, and CaCl2 2 mmol/L, and the pH of the extracellular fluid was adjusted to be equal to 7.25 at the time of use by NaOH solution at a concentration of 1.2 mmol/ L and saturated with a 97% O2/3% CO2 gas mixture for about 20 min prior to application, and the extracellular fluid was filtered through a 0.21 pm filter membrane.

Artificial cerebrospinal fluid with delayed rectifier K+ channel current was recorded. CdCl2 0.2 mmol/L, TTX 4 mmol/L, and 4-AP 3 mmol/L were injected into the artificial cerebrospinal fluid.

Transient outward K+ channel currents were recorded in artificial cerebrospinal fluid. CdCl2 0.2 mmol/L, TEA-C1 2 mmol/L, and TTX 3 mmol/L were added to the artificial cerebrospinal fluid.

III. A. 2) Acoustic stimulation systems

To prevent interference from external acoustic stimuli, the entire electrophysiologic recording in this study was performed in an electroacoustically shielded room (M Auditory Speech Technology Ltd.). The generation of acoustic stimuli and the processing of neuroelectric signals were performed on the TDT neurophysiological workstation system. The acoustic stimuli were generated and output by a multi-function processor (RX) device and transmitted through a stereo amplifier to a closed-field magnetic loudspeaker headphone in the electroacoustic shielding room, and an adapter tube that fit the size of the external ear canal of the rats was installed in the front of the headphone, so that the acoustic stimuli were delivered to the rats' ears on both sides via the MF of the headphone and the adapter tubes. Before the whole experiment, the closed-field magnetic loudspeaker headphones with adapter tubes were calibrated in the frequency range of 1.8 kHz - 45 kHz, and the intensity of the sound emitted by the headphones was calibrated at different frequencies to ensure the accuracy of the frequency and intensity of the sound given in the experiment. In the experiment, rats were given sequential acoustic stimuli of different intensities in the left and right ears using headphones to simulate the sound of movement.

In this study, the acoustic stimuli given to the rats were pure tone stimuli with a frequency range of 3.8 kHz - 45 kHz, and the duration of each individual acoustic stimulus in a sequence of acoustic stimuli was 30 ms, with a rise and fall time of 2 ms. Fig. 3 shows the schematic diagram of the acoustic stimuli to simulate the locomotion sound. In the design of motion sound composed of multiple acoustic stimuli, we varied the speed of the motion sound by changing the binaural intensity difference (ILD in dB) of the intensity of neighboring acoustic stimuli as well as the time between neighboring acoustic stimuli, and simulated the motion of the sound along the horizontal azimuth from one side to the other by the change of the binaural intensity difference, and the unit of the motion speed was dB/s accordingly.

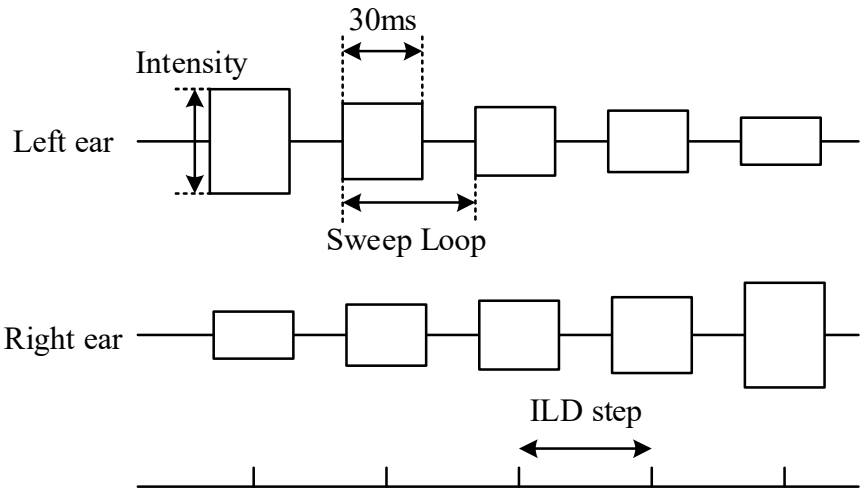

Figure 3: Schematic diagram of acoustic stimulation for simulating motion sounds

Due to the programming conditions of the TDT device, we modified the binaural intensity difference step size to 15 dB for the 60 dB/s and 40 dB/s conditions, and the adjacent acoustic stimulus intervals to 120 ms and 180 ms, respectively. The simulated motion sound directions were divided into left-to-right and right-to-left, and the combinations of these different conditions were arranged in such a way that the binaural average intensity (ABL) was selected to be 60 dB versus 80 dB. The combinations of acoustic stimuli with different motion directions and

motion speeds were repeated 20 times. The combinations of acoustic stimuli with different motion directions, acoustic stimulus intensities, and motion speeds were repeated 20 times.

III. B. Experimental Methods

III. B. 1) Cortical neuron preparation

The brains of 8~15-day-old SD mice were severed from their heads, quickly stripped out and submerged in artificial cerebrospinal fluid (ASF) at 0~5℃ for 2 min. After that, the cortex of the mice was detached on an ice pillow, and the brain slices were cut manually into 500~700 μm slices and placed in ASF with a continuous 97%O2/3%CO2 gas mixture, and the brain slices were incubated in ASF for 40 min. After incubation for 40 min, Pronase was added to a final concentration of 0.25 g/L, and the slices were digested at 31℃ for 20 min, then rinsed with incubation solution for 3~5 times, and then continued to be incubated in artificial cerebrospinal fluid with 97% O2/3% CO2 for about 60 min before they were ready to be used for experiments, and the slices were able to maintain good physiological status within 3~7 hours.

Take 2-3 brain slices into the centrifuge tube containing artificial cerebrospinal fluid, gently blow with Pasteur pipettes of different caliber to make cell suspension, take the upper part of the cell suspension after 3~4 min of resting, put it into the petri dish with coverslip, and after the cells are attached to the wall for 30 min, use the standard extracellular fluid to flush 1~2 times, then it can be used for the whole-cell membrane-clamp recording.

III. B. 2) Methods of electrophysiologic recording

According to the cell characteristics and experimental requirements, electrophysiological recordings in this experiment were performed by whole-cell membrane clamp. The borosilicate glass capillaries were pulled into electrodes using a microelectrode puller, and the synaptic currents were recorded by EPC amplifiers. The specific steps are as follows:

Recording of mini-EPSC. mini-EPSC is a microsmall excitatory postsynaptic current spontaneously released by a single vesicle in a nerve cell.

(1) Maintain the laboratory temperature at about 31°C. Action potentials were blocked by adding 1.2 μM GABA-A receptor blocker PTX and 1 μM TTX to the extracellular fluid.

(2) Mature neurons cultured in vitro were transferred to the cell bath containing extracellular fluid on the carrier stage of the membrane-clamp amplification system, and the cells were found to be stereochemically full under the microscope.

(3) Fill the electrode with the internal fluid, flick it to remove air bubbles, and secure the electrode to the electrode holder; close the three-way valve immediately after blowing to give a positive pressure before filling the fluid. After liquid entry, the electrode resistance was made to vary between 4 and 6 MOhm. Both the end of the electrode and the cell were placed in the center of the field of view under the lens.

(4) Slowly lower the electrode, and when the electrode contacts the cell membrane and the resistance rises by about 0.3 MOhm, clamp the voltage at -12 mV, and lightly inhale to clamp the voltage at -80 mV. When the resistance was about 220 MOhm, the three-way valve was opened and the resistance rose to GOhm and was maintained for 2 min. The membrane was broken and compensated by light suction and waited for 2 min to allow the electrode internal fluid to diffuse fully into the cell. Recording was then started.

evoked-EPSC records. evoked-EPSC is an excitatory postsynaptic current released by nerve cells evoked by specific electrical stimulation. QX was added to the intracellular fluid and PTX to the extracellular fluid. The method of clamping the cells was the same as above. The difference is that, before the glass electrode into the liquid, you need to put a stimulation electrode next to the cell, set the stimulation parameters current intensity of 80 μA, stimulation frequency of 0.05 Hz, stimulation time of 2 ms. when recording, open the stimulator, and then record the data.

IV. Findings and analysis

Ion channels are transmembrane proteins that selectively mediate the flow of ions across the lipid bilayer and are the basis for bioelectrical activity. Taking nerve and cardiomyocytes as an example, more than half of the current nerve and cardiac drugs act on specialized ion channels on these cells. Thus, the study of ion channels is indispensable to the understanding of cell function and the invention of effective drugs for the treatment of many serious diseases.

IV. A. Effects on I-V curves of ion channels

IV. A. 1) Sodium channel current I-V curve

Using the extracellular fluid and sodium electrode internal fluid prepared previously, Ca2+ current and K+ current on mouse brain cortical neurons were blocked by the addition of 5 mmol/L 4-AP, 0.15 mmol/L CdCl2, and 35 mmol/L

TEA-Cl, respectively, to the whole-cell standard extracellular fluid, and voltage-gated Na+ channel currents were recorded on the membranes of individual cortical nerve cells. A depolarizing pulse with an amplitude of -120mV~+50mV, a step size of +15mV, and a pulse width of 15ms was given, and the clamp potential was -110mV. 12 cells with good morphological observation were selected from both the control group and the different exposure groups to record Na+ currents. The I-V curves of Na+ channel currents were plotted as shown in Fig. 4, using different membrane potentials (depolarizing stimulus potentials) as the horizontal axis, and the value of Na+ channel current density (current/membrane capacitance) activated at this membrane potential as the vertical axis. Table 1 shows the maximum peak current densities of ion channel currents at different noise stimulation times, and * in the table indicates that both IA and IK peak current densities decreased significantly at different noise stimulation times ($P<0.05$).

The activation and peak potentials of the Na+ channel I-V curves in the noise-stimulated group were shifted to the left, and both the activation and peak potentials were shifted left by about -15 mV compared with the control group. From the I-V curves, it can be concluded that the external noise environment can increase the peak Na+ channel current density. The peak current density increased significantly when the external noise environment acted for 6, 12 and 18 min ($P<0.05$). The results showed that the external noise environment could significantly affect the Na+ channel current with time dependence, and the current basically stabilized after 12 min of exposure to the external noise environment.

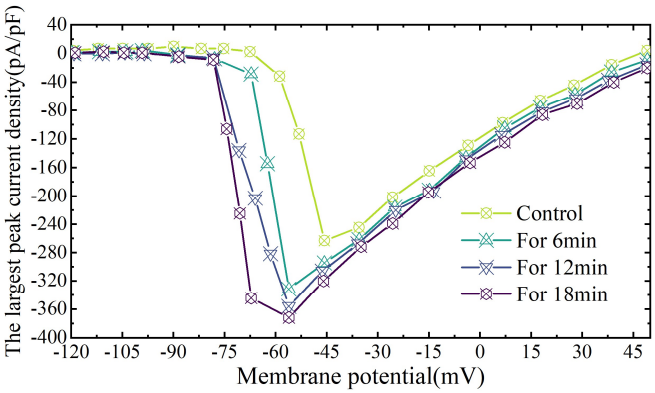

Figure 4: Na+ channel current

Table 1: The largest peak current density(pA/pF)

Time (min)	Na+ current density	IA current density	IK current density
Control (0)	-263.22±38.47	222.69±38.75	192.35±28.92
For 6 min	-331.79±25.12	121.42±25.63	151.73±23.24
For 12 min	-356.07±16.38	102.71±16.89	122.84±16.35
For 18 min	-372.83±11.09	83.24±11.27	78.49±12.06

IV. A. 2) Instantaneous outward potassium current I-V curve

The sodium current, calcium current, and delayed rectifier potassium current of neuronal ion channels in the mouse cerebral cortex were blocked by using K+ channel electrode internal fluid and whole-cell standard extracellular fluid, and 2 μmol/L TTX tetrodotoxin, 0.15 mmol/L CdCl2, and 25 mmol/L TEA-Cl were added to the external fluid. A set of transient outward potassium currents was obtained by placing the clamp potential at -90 mV and giving depolarizing pulses with amplitudes of -50 mV to +40 mV, widths of 50 ms, and steps of 12 mV. The I-V curve of IA was plotted as shown in Fig. 5, using the membrane potential as the horizontal axis and the value of IA current density (maximum current/membrane capacitance) activated at this membrane potential as the vertical axis. The correlation test is shown in Table 1 before.

There was a significant decrease in IA at 6, 12 and 18 min of external noise stimulation effect ($P<0.05$). From the I-V curve, external noise stimulation could inhibit the transient outward potassium current of ion channel, and the percentage of inhibition was 45.48%, 53.88%, and 62.62% at 6min, 12min, and 18min of external noise stimulation effect, respectively ($P<0.05$). The experimental results showed that external noise stimulation significantly inhibited the transient outward potassium current IA in a time-dependent manner.

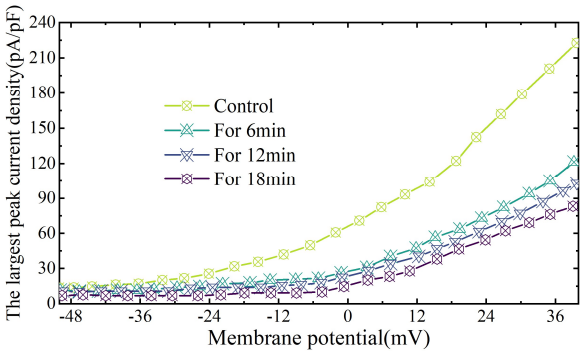

Figure 5: Transient outward potassium channel current

IV. B. Effect of noise stimuli on Na+ ion channel properties

IV. B. 1) Na+ ion channel activation curves

From the I-V curve, the membrane potential of ion channel activation can be roughly reflected, but it is very imprecise. In order to further study the correlation between the ion channel activation characteristics, the voltage dependence of the stimulus effect of the external noise and the state of the ion channel, it is necessary to determine the steady-state activation curve of the channel. The parameter settings were similar to those of the I-V curve determination, and the stimulation time was generally set to be relatively long in order to ensure that the whole process of steady state activation was observed. When different membrane potential depolarizing stimuli were applied, the ratio of the recorded current at each voltage to the current at maximum activation was plotted against each membrane potential to obtain the steady-state activation curve, which was consistent with the Boltzmann distribution. By studying the activation curve, it can be determined whether the industrial frequency magnetic field affects the activation process of sodium channels.

The membrane potential was clamped to -120 mV, and the hyperpolarizing voltage of -100 mV was preconditioned for 400 ms, and then a depolarizing pulse stimulation with 20 mV step increments and 15 ms wavewidth was given from -100 mV to 10 mV, and the stimulation frequency was 0.25 Hz, and a series of fast inactivation and fast activation of sodium currents were induced as a control. Current values were converted to conductance values using the formula. The ratio of conductance value to maximum conductance value, G/Gmax, was used to correspond to the membrane potential, and the steady-state activation curves of Na+ currents before and after the effect of external noise stimulation were plotted as shown in Figure 6, respectively.

The resulting curve can be fitted with the Boltzmann equation $G/G_{\max}=1/\{1+\exp[V-V_{1/2}]/k\}$, where $V_{1/2}$ is the half-activation voltage, and k is the slope factor of the curve. As can be seen from the figure, the activation curves of both the control and external noise stimulation groups were S-shaped, and from this, the half-activation voltages $V_{1/2}$ of the inward Na+ currents in the control and external noise stimulation groups were calculated to be -32.04±0.58 mV and -56.42±0.51 mV, respectively ($P<0.05$), and the slope factors k were 5.71±0.32 mV and 7.28±0.53mV ($P<0.05$). It can be seen that the external noise stimulation effect changed the activation process of Na+ ion channel currents, shifted the steady-state activation curve to the left, and changed its slope factor. This suggests that the external noise stimulation effect promotes the activation process of the Na+ current, which leads to the advancement of the opening of the voltage-gated Na+ channel.

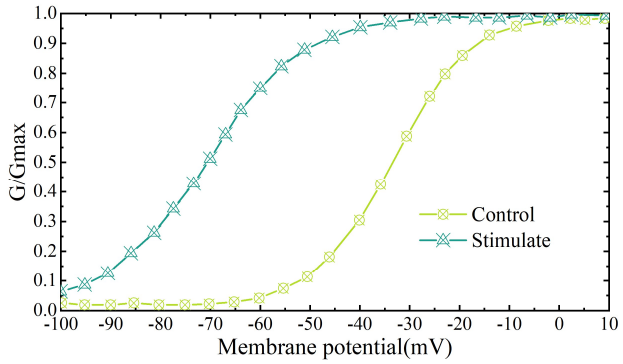

Figure 6: Steady-state activation curve of Na+ current

IV. B. 2) Na+ ion channel inactivation curves

For the study of inactivation curves the external noise dual stimulation method is generally used, where a series of external noise stimuli are first applied, followed immediately after each external noise stimulus by a fixed depolarizing external noise. The duration of each external noise is sufficiently long to completely inactivate the channel being measured, while the test external noise is used to record the activity of the portion of the channel that is not inactivated. The ratio of the recorded membrane current to the current at maximum activation is plotted against the corresponding membrane potential to obtain an inactivation curve, which also conforms to the Boltzmann distribution. The inactivation curve can be used to illustrate the voltage dependence of channel inactivation and the effect of external noise stimulation on channel inactivation. When the external noise stimulus affects the process of channel inactivation in a voltage-dependent manner, the inactivation curve will be shifted to the left or right, or the slope factor of the curve will be changed.

A clamp potential of -120 mV was set, and a step-clamp external noise stimulus of -100 to -10 mV with a step size of +15 mV and a stimulus waveform width of 400 ms was first given, and after an interval of 2 ms, a test external noise stimulus of -40 mV was given, with a stimulus waveform width of 10 ms and a stimulus frequency of 0.3 Hz, and the resulting current was recorded as a control. The steady-state inactivation curves of Na+ currents in the control and external noise stimulation groups were plotted in terms of the ratio of the peak current to the maximum peak current, I/Imax, corresponding to the external noise stimulation potentials as shown in Fig. 7, respectively. The resulting curves can be fitted with the Boltzmann equation $I / I_{\max} = 1 / \{1 + \exp[V - V_{1/2}] / k\}$, where I is the peak current, V is the membrane potential, $V_{1/2}$ is the half of the inactivation voltage, and k is the slope factor of the curve.

From the figure, it can be seen that the inactivation curves of both the control and external noise stimulation groups were in inverse S-shape, and from this, the half inactivation voltages of Na+ currents in the control and external noise stimulation groups were calculated as $V_{1/2}$ were -30.21±0.19mV and -50.52±0.75mV, respectively (P<0.05), and the slope factors k were 10.34± 1.16mV and 9.24±0.84mV (P<0.05). It can be seen that external noise stimulation can promote the inactivation of Na+ ion channel current and shift the inactivation curve in the direction of hyperpolarization, which makes the inactivation of voltage-gated Na+ ion channel faster.

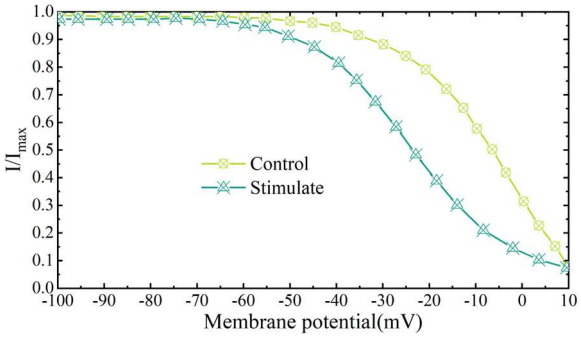

Figure 7: The steady-state deactivation curve of Na+ current

IV. B. 3) Bifurcation Mechanism for Oscillatory Positive Feedback

In order to study the kinetics of transitions between different ions of the ion channel under external noise stimulation, including those of Na+ and K+, we obtained a two-parameter bifurcation mechanism using [Na+] and [K+] as the bifurcation parameters. Based on the H-H model given in the previous section, it can be seen that the transfer of mixed ions from the oscillatory phase to the depolarization block is related to the supercritical Hopf bifurcation (HB), the transfer from the depolarization block phase to the rest phase is related to the saddle-node bifurcation, and the transfer from the rest phase to the cluster oscillatory phase is related to the saddle-node-on-current-invariant-circle (SNIC) bifurcation.

Figure 8 shows the positive feedback bifurcation mechanism of cortical neurons oscillating in mixed ions under the effect of external noise stimulation, in which Figures 8(a)~(c) show the amplification results of the oscillatory phase of the anomalous mixed ions, the transient discharge frequency, and the superimposed results of the single-parameter bifurcation, respectively.

From the figure, it can be seen that the [Na+] level is elevated, then the membrane potential level is elevated, and the increase in the discharge frequency forms a continuous positive feedback, which leads to the elevation of the membrane potential level (with a narrowing of the amplitude of the oscillation), and enters into the depolarization block phase, which is the kinetic process of the mixed-ion generation. In Fig. 8(c), with the increase of [Na+], the

mixed-ion system enters the discharge state (thick black solid line above and below) from the resting state (thin black solid line on the left) via the SNIC bifurcation, and subsequently enters the depolarization block state (thin black solid line on the right) with high membrane potential via the HB bifurcation. The projected trajectories (green) of the cluster oscillation phase in the phase plane show the following relationship with the bifurcation: the phase trajectories oscillate along the stabilization limit loop, i.e., the membrane potential is lifted and oscillation amplitude is reduced, and the frequency of oscillation is increased, via the SNIC bifurcation, and reach the HB bifurcation. Crossing the HB bifurcation, it runs along the stable equilibrium point after the critical slow-change effect of the Hopf bifurcation (small amplitude oscillations on the right side of the HB), forming a depolarizing block. Therefore, the positive feedback is related to the limit loop between the SNIC and the HB bifurcation, and the amplitude and frequency of the mixed ion oscillations are close to the limit loop.

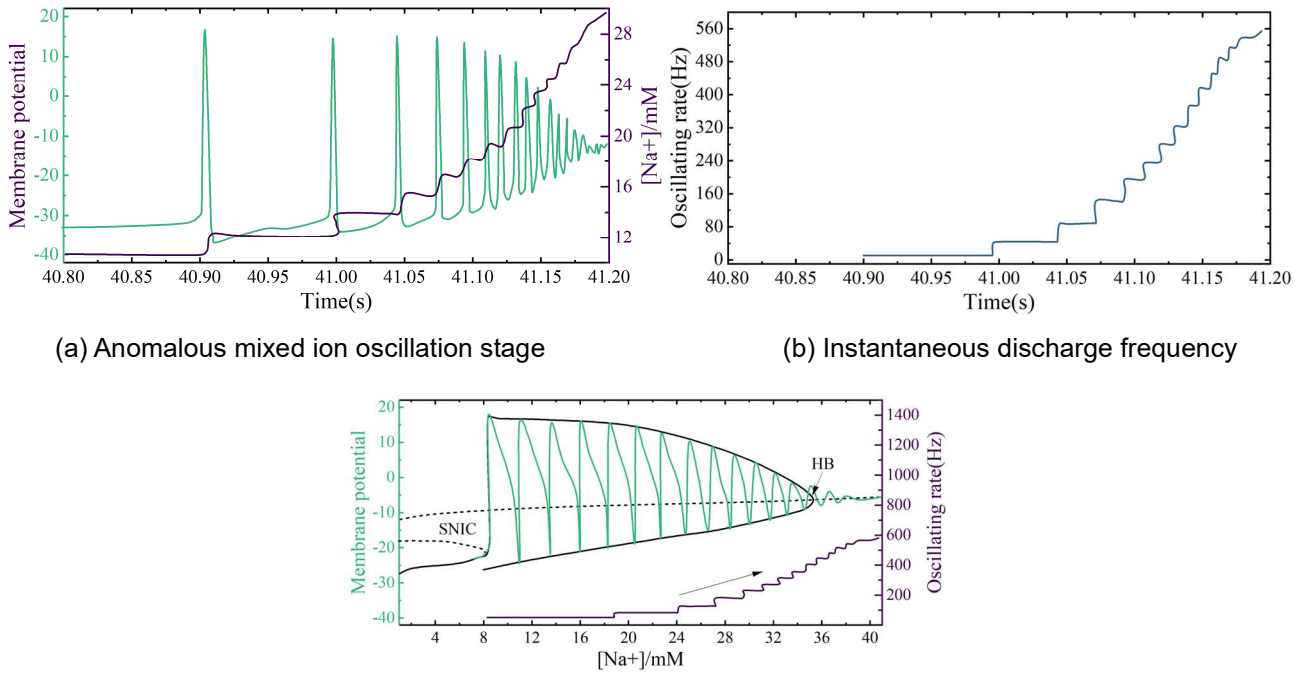

(a) Anomalous mixed ion oscillation stage

(b) Instantaneous discharge frequency

(c) Superposition of single-parameter bifurcations

Figure 8: The bifurcation mechanism of oscillatory positive feedback

V. Conclusion

External noise stimulation significantly altered the ion channel properties of cortical neurons. Electrophysiological experiments demonstrated that noise stimulation caused an increase in Na+ channel current density, which increased to -372.83 ± 11.09 pA/pF after 18 min of stimulation, an increase of 41.64% compared with the control group. Meanwhile, noise stimulation significantly inhibited the transient outward potassium current I_1, and the inhibitory effect was time-dependent, with 62.62% inhibition at 18 min. Ion channel kinetic analysis showed that noise stimulation promoted the activation process of Na+ channels, shifting the half activation potential of Na+ channels by 24.38 mV toward hyperpolarization; at the same time, it accelerated the inactivation process of Na+ channels, with the half inactivation potential shifted leftward by 20.31 mV. These changes collectively led to advancement of the opening probability of Na+ channels, which in turn affected the excitability of neurons. Two-parameter bifurcation analysis revealed that neuronal oscillatory properties are jointly regulated by Na+ and K+ dynamics, and that noise stimulation induces changes in the frequency and amplitude of oscillatory discharges by altering the properties of the ion channels, involving both SNIC bifurcation and HB bifurcation processes. This finding provides a mechanistic explanation at the cellular and molecular levels for understanding the effects of the noise environment on the function of the nervous system, and is of great significance in guiding the development of non-invasive neuromodulation techniques based on acoustic stimulation.

Ethical Compliance

All procedures performed in this study involving human participants were in accordance with the ethical standards of the institutional and/or national research committee and with the 1964 Helsinki Declaration and its later amendments or comparable ethical standards.

Data Access Statement

Research data supporting this publication are available from the NN repository at www.NNN.org/download/.

Conflict of Interest Declaration

The authors declare that they have no affiliations with or involvement in any organization or entity with any financial interest in the subject matter or materials discussed in this manuscript.

Funding

This study was supported by the General Project for Outstanding Youth Talent Support Program in Universities of Anhui Province of China (gxyq2022186); the University Youth Teacher Training Action Project of Anhui Province of China (YQZD2024065); the Key Project of University Natural Science Research of Anhui Province of China (2023AH053238); and the major Foundation of University Natural Science Research of Anhui Province of China (KJ2019ZD64).

References

[1] Sousa, A. M., Meyer, K. A., Santpere, G., Gulden, F. O., & Sestan, N. (2017). Evolution of the human nervous system function, structure, and development. Cell, 170(2), 226-247.
[2] Breakspear, M. (2017). Dynamic models of large-scale brain activity. Nature neuroscience, 20(3), 340-352.
[3] Ma, J., & Tang, J. (2017). A review for dynamics in neuron and neuronal network. Nonlinear Dynamics, 89, 1569-1578.
[4] Allen, N. J., & Lyons, D. A. (2018). Glia as architects of central nervous system formation and function. Science, 362(6411), 181-185.
[5] Demirtaş, M., Burt, J. B., Helmer, M., Ji, J. L., Adkinson, B. D., Glasser, M. F., ... & Murray, J. D. (2019). Hierarchical heterogeneity across human cortex shapes large-scale neural dynamics. Neuron, 101(6), 1181-1194.
[6] Singer, W. (2018). Neuronal oscillations: unavoidable and useful?. European Journal of Neuroscience, 48(7), 2389-2398.
[7] Riddle, J., & Frohlich, F. (2021). Targeting neural oscillations with transcranial alternating current stimulation. Brain research, 1765, 147491.
[8] Raja, V. (2018). A theory of resonance: Towards an ecological cognitive architecture. Minds and Machines, 28, 29-51.
[9] Baysal, V., & Calim, A. (2023). Stochastic resonance in a single autapse–coupled neuron. Chaos, Solitons & Fractals, 175, 114059.
[10] Calim, A., Palabas, T., & Uzuntarla, M. (2021). Stochastic and vibrational resonance in complex networks of neurons. Philosophical Transactions of the Royal Society A, 379(2198), 20200236.
[11] Xu, Y., Guo, Y., Ren, G., & Ma, J. (2020). Dynamics and stochastic resonance in a thermosensitive neuron. Applied Mathematics and Computation, 385, 125427.
[12] Helfrich, R. F., Breska, A., & Knight, R. T. (2019). Neural entrainment and network resonance in support of top-down guided attention. Current opinion in psychology, 29, 82-89.
[13] Zhang, Y., Xu, Y., Yao, Z., & Ma, J. (2020). A feasible neuron for estimating the magnetic field effect. Nonlinear Dynamics, 102(3), 1849-1867.
[14] Van der Groen, O., Potok, W., Wenderoth, N., Edwards, G., Mattingley, J. B., & Edwards, D. (2022). Using noise for the better: The effects of transcranial random noise stimulation on the brain and behavior. Neuroscience & Biobehavioral Reviews, 138, 104702.
[15] Keil, J., & Senkowski, D. (2018). Neural oscillations orchestrate multisensory processing. The Neuroscientist, 24(6), 609-626.
[16] Guo, D., Perc, M., Liu, T., & Yao, D. (2018). Functional importance of noise in neuronal information processing. Europhysics Letters, 124(5), 50001.
[17] Iemi, L., Gwilliams, L., Samaha, J., Auksztulewicz, R., Cycowicz, Y. M., King, J. R., ... & Haegens, S. (2022). Ongoing neural oscillations influence behavior and sensory representations by suppressing neuronal excitability. NeuroImage, 247, 118746.
[18] Wang, R., Feng, P., Fan, Y., & Wu, Y. (2019). Spontaneous electromagnetic induction modulating the neuronal dynamical response. International Journal of Bifurcation and Chaos, 29(01), 1950005.
[19] Mehwish Akram, Christina Kadi, Eleanor Parker, Claire Brown, Laura Pisarek, Simon Rice... & Laura Hutchison. (2025). BPS2025 - Functional characterization of GRIN2B variants using automated patch clamp technology. Biophysical Journal,124(3S1),464a-465a.
[20] Maria G. Rotordam, Nadine Becker, Timothy Strassmaier, Søren Friis, Alison Obergrussberger, Michael George & Niels Fertig. (2025). BPS2025 - Investigating the effect of temperature and trafficking modulators on hERG current using high throughput automated patch clamp. Biophysical Journal,124(3S1),277a-277a.
[21] Young Soo Lim, Ji Hong Kim, Junho Kim, MinhDuc Hoang, Wonok Kang, Mattew Koh... & Sung Min Park. (2025). Precise control of tibial nerve stimulation for bladder regulation via evoked compound action potential feedback mechanisms. Nature Communications,16(1),4115-4115.
[22] Divya Govindaraju, Sutha Subbian & S Nambi Narayanan. (2025). Computational modelling for risk assessment of neurological disorder in diabetes using Hodgkin-Huxley model. Computer methods and programs in biomedicine,267,108799.
[23] Holford Jacob J., Lee Myoungkyu & Hwang Yongyun. (2023). Optimal white-noise stochastic forcing for linear models of turbulent channel flow. Journal of Fluid Mechanics,961(432), A32-A32.